Targeting DNA with Novel Diphenylcarbazoles†

Nathalie Dias,‡ Ulrich Jacquemard,§ Brigitte Baldeyrou,‡ Christelle Tardy,‡ Amélie Lansiaux,‡ Pierre Colson,|| Farial Tanious,⊥ W. David Wilson,⊥ Sylvain Routier,§ Jean-Yves Mérour,§ and Christian Bailly*,‡

INSERM U-524 et Laboratoire de Pharmacologie Antitumorale du Centre Oscar Lambret, IRCL, 59045 Lille, France, Institut de Chimie Organique et Analytique, UMR 6005, associé au CNRS, Université d'Orléans, B.P. 6759, 45067 Orléans Cedex 2, France, Biospectroscopy and Physical Chemistry Unit, Department of Chemistry and Natural and Synthetic Drugs Research Center, University of Liege, Sart-Tilman, 4000 Liege, Belgium, and Department of Chemistry and Laboratory for Chemical and Biological Sciences, Georgia State University, Atlanta, Georgia 30303

Received July 17, 2004; Revised Manuscript Received September 26, 2004

ABSTRACT: Double-stranded DNA is a therapeutic target for a variety of anticancer and antimicrobial drugs. Noncovalent interactions of small molecules with DNA usually occur via intercalation of planar compounds between adjacent base pairs or minor-groove recognition by extended crescent-shaped ligands. However, the dynamic and flexibility of the DNA platform provide a variety of conformations that can be targeted by structurally diverse compounds. Here, we propose a novel DNA-binding template for construction of new therapeutic candidates. Four bisphenylcarbazole derivatives, derived from the combined molecular architectures of known antitumor bisphenylbenzimidazoles and anti-infectious dicationic carbazoles, have been designed, and their interaction with DNA has been studied by a combination of biochemical and biophysical methods. The substitutions of the bisphenylcarbazole core with two terminal dimethylaminoalkoxy side chains strongly promote the interaction with DNA, to prevent the heat denaturation of the double helix. The deletion or the replacement of the dimethylamino-terminal groups with hydroxyl groups strongly decreased DNA interaction, and the addition of a third cationic side chain on the carbazole nitrogen reinforced the affinity of the compound for DNA. Although the bi- and tridentate molecules both derive from well-characterized DNA minor-groove binders, the analysis of their binding mode by means of circular and linear dichroism methods suggests that these compounds form intercalation complexes with DNA. Negative-reduced dichroism signals were recorded in the presence of natural DNA and synthetic AT and GC polynucleotides. The intercalation hypothesis was validated by unwinding experiments using topoisomerase I. Prominent gel shifts were observed with the di- and trisubstituted bisphenylcarbazoles but not with the uncharged analogues. These observations, together with the documented stacking properties of such molecules (components for liquid crystals), prompted us to investigate their binding to the human telomeric DNA sequence by means of biosensor surface plasmon resonance. Under conditions favorable to G4 formation, the title compounds showed only a modest interaction with the telomeric quadruplex sequence, comparable to that measured with a double-stranded oligonucleotide. Their sequence preference was explored by DNase I footprinting experiments from which we identified a composite set of binding sequences comprising short AT stretches and a few other mixed AT/GC blocks with no special AT character. The variety of the binding sequences possibly reflects the coexistence of distinct positioning of the chromophore in the intercalation sites. The bisphenylcarbazole unit represents an original pharmacophore for DNA recognition. Its branched structure, with two or three arms suitable to introduce a structural diversity, provides an interesting scaffold to built molecules susceptible to discriminate between the different conformations of nucleic acids.

Recently, a series of head−head bisphenylbenzimidazoles was identified as a promising new class of antitumor agents (*1*). The potent cytotoxic activity of these compounds was associated with their capacity to bind selectively to AT-rich sequences in the minor groove of DNA. These molecules selectively recognize blocks of four consecutive A−T base pairs via water-mediated drug−DNA interactions (*2*) or longer sequences, such as the $[A{\cdot}T]_4-[G{\cdot}C]-[A{\cdot}T]_4$ motif, when they are dimerized (*3*). The most potent compounds in this series corresponded to those substituted with hydroxy groups or dimethylaminoalkoxy side chains. In particular, the two bisphenylbenzimidazole compounds shown in Figure 1 have revealed *in vivo* activity against an ovarian cancer model in mice (*1*). In a subsequent study, the same amino compound (ABA833) has shown pronounced and selective antiproliferative activities against several breast carcinoma cell lines (*4*). The therapeutic potential of these molecules

† This work was supported by grants (to C.B.) from the Ligue Nationale Contre le Cancer (Comité du Nord) and the Institut de Recherches sur le Cancer de Lille, (to S.R.) from the Ligue Nationale Contre le Cancer (Comité du Centre), and (to W.D.W.) from the National Institutes of Health (NIH Grant GM61587), the Georgia Research Alliance and a Gates Foundation Grant. N.D. is the recipient of a fellowship from the Ligue Nationale Contre le Cancer. Support by the "Actions intégrées Franco-Belge, Programme Tournesol" is acknowledged.

* To whom correspondence should be addressed: INSERM U-524, IRCL, Place de Verdun, 59045 Lille, France. Fax: +33-320-16-92-29. E-mail: bailly@lille.inserm.fr.

‡ INSERM U-524.

§ Université d'Orléans.

|| University of Liege.

⊥ Georgia State University.

10.1021/bi048474o CCC: $27.50
Published on Web 11/09/2004

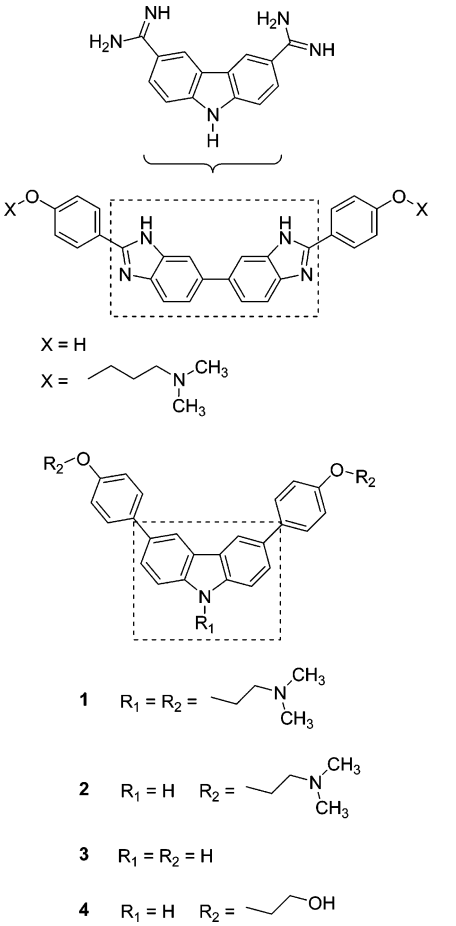

FIGURE 1: Structures of the drugs mentioned in this study.

prompted us to design a series of related compounds for which the central bisbenzimidazole unit has been replaced with a carbazole core. The reason for the choice of this planar tricyclic system derives from our long-term interest in the chemistry of indoles and carbazoles (*5*, *6*) coupled with the known capacity of certain 3,6-disubstituted carbazoles to recognize preferentially AT-rich DNA sequences. Indeed, a high AT selectivity can be achieved with 3,6- (and 2,7-) substituted diamidino and bisimidazolidine carbazoles, which also have a potential therapeutic value for the treatment of opportunistic infections (*7*−*9*). These carbazole and bisbenzimidazole compounds are believed to exert their biological action via tight binding to AT sequences in the minor groove of DNA and subsequent inhibition of DNA-directed enzymes, possibly helicases (*10*) but not topoisomerases (*4*).

Various bisphenylcarbazole derivatives substituted with polar side chains have been synthesized (*11*), and here, we report the results of our pharmacological study aimed at elucidating, at least partially, the molecular mechanism of action of these compounds. Four molecules (**1**−**4** in Figure 1) were selected, and their DNA-binding properties were investigated by means of complementary biochemical and biophysical methods to compare their relative DNA-binding affinity, mode of DNA interaction, and sequence selectivity.

MATERIALS AND METHODS

Chemicals and Biochemicals. The synthesis of the diphenylcarbazoles together with their cytotoxic properties will be reported separately (*11*). Camptothecin and etoposide were from Aldrich. The drugs were dissolved in DMSO at 5 mM. The stock DMSO solutions of drugs were kept at −20 °C and freshly diluted with water to the desired concentration immediately prior to use.

Absorption Spectroscopy and Melting Temperature Studies. Absorption spectra and melting curves were measured using an Uvikon 943 spectrophotometer coupled to a Neslab RTE111 cryostat. Titrations of the drug with DNA, covering a large range of DNA−phosphate/drug ratios (P/D), were performed by adding aliquots of a concentrated DNA to a ligand solution at a constant concentration (20 μM). The T_m measurements were performed in BPE buffer at pH 7.1 (6 mM Na_2HPO_4, 2 mM NaH_2PO_4, and 1 mM EDTA). The temperature inside the cuvette (10 mm path length) was increased over the range 30−100 °C with a heating rate of 1 °C/min. The "melting" temperature T_m was taken as the midpoint of the hyperchromic transition.

Circular Dichroism (CD). CD spectra were recorded on a J-810 Jasco dichrograph. Solutions of drugs, nucleic acids, and their complexes (1 mL in 1 mM sodium cacodylate buffer at pH 7.0) were scanned in 1 cm quartz cuvettes. Measurements were made by progressive dilution of the drug−DNA complex at a high P/D (phosphate/drug) ratio with a pure ligand solution to yield the desired drug/DNA ratio. Three scans were accumulated and automatically averaged.

Electric Linear Dichroism (ELD). Poly(dAT)$_2$ and poly(dGC)$_2$ were purchased from Sigma. Calf thymus DNA (Pharmacia) was deproteinized with sodium dodecyl sulfate (SDS) (protein content < 0.2%). All nucleic acids were extensively dialyzed against 1 mM sodium cacodylate buffered solution at pH 7.0 prior to the ELD measurements performed with a computerized optical measurement system using the procedures previously outlined (*12*). All experiments were conducted with a 10 mm path-length Kerr cell having a 1.5 mm electrode separation. The samples were oriented under an electric field strength varying from 1 to 14 kV/cm. Unless specified, 10 μM of the tested drug was incubated with 200 μM of DNA. This electro-optical method senses only the orientation of the polymer-bound ligand; free ligand is isotropic and does not contribute to the signal (*13*).

DNase I Footprinting. The complete procedure has been recently detailed (*14*). The 265-bp DNA fragment was prepared by 3′-[^{32}P]end labeling of the *Eco*RI−*Pvu*II double digest of the pBS plasmid (Stratagene) using α-[^{32}P]dATP (Amersham, 3000 Ci/mmol) and AMV reverse transcriptase (Roche). The labeled digestion products were separated on a 6% polyacrylamide gel under nondenaturing conditions in Tris-borate-EDTA (TBE)[1] buffer (89 mM Tris-borate at pH 8.3 and 1 mM EDTA). After autoradiography, the requisite band of DNA was excised, crushed, and soaked in water overnight at 37 °C. This suspension was filtered through a Millipore 0.22 μm filter, and the DNA was precipitated with ethanol. The labeled DNA was then washed with 70% ethanol, vacuum-dried, and resuspended in a solution containing 10 mM Tris at pH 7.0 and 10 mM NaCl.

Bovine pancreatic deoxyribonuclease I (DNase I, Sigma Chemical Co.) was stored as a 7200 units/mL solution in 20 mM NaCl, 2 mM $MgCl_2$, and 2 mM $MnCl_2$ at pH 8.0. The

[1] Abbreviations: SPR, surface plasmon resonance; TBE, Tris-borate-EDTA.

stock solution of DNase I was kept at −20 °C and freshly diluted to the desired concentration immediately prior use. Footprinting experiments were performed essentially as previously described (*15*). Briefly, reactions were conducted in a total volume of 10 μL. Samples (2 μL) of the labeled DNA fragments were incubated with 6 μL of the buffered solution containing the ligand at the appropriate concentration. After incubation for 10 min at room temperature to ensure equilibration of the binding reaction, the digestion was initiated by the addition of 2 μL of a DNase I solution whose concentration was adjusted to yield a final enzyme concentration of about 0.03 unit/mL in the reaction mixture. After 3 min, the reaction was stopped by freeze drying. Samples were lyophilized and resuspended in 5 μL of a 80% formamide solution containing the tracking dyes. The DNA samples were then heated at 90 °C for 4 min and chilled in ice for 4 min prior to loading.

DNA cleavage products were resolved by polyacrylamide gel electrophoresis under denaturating conditions (8% acrylamide containing 7 M urea). After electrophoresis (about 2 h at 60 W in TBE-buffered solution), gels were soaked in 10% acetic acid for 10 min, transferred to a Whatman 3MM paper, and dried under vacuum at 80 °C. A Molecular Dynamics 425E PhosphorImager was used to collect data from the storage screens exposed to dried gels overnight at room temperature. Baseline-corrected scans were analyzed by integrating all of the densities between two selected boundaries using ImageQuant version 3.3 software. Each resolved band was assigned to a particular bond within the DNA fragments by comparison of its position relative to sequencing standards generated by treatment of the DNA with dimethyl sulfate followed by piperidine-induced cleavage at the modified guanine bases in DNA (G track).

Biosensor Surface Plasmon Resonance (SPR) Binding Studies. BIAcore 2000 SPR measurements were performed with four channel streptavidin-coated sensor chips (SA). To prepare sensor chips for use, they were conditioned with three consecutive 1-min injections of 1 M NaCl in 50 mM NaOH followed by extensive washing with buffer. 5′-Biotinylated DNA samples (human G4, 5′-biot-d[$AG_3(TTAG_3)_3$] and a duplex, 5′-biot-d[CGAATTCG-TCTC-CGAATTCG]) in Hepes buffer at pH 7.4 [0.01 M Hepes, 0.15 M NaCl, 3 mM EDTA, and 0.005% (v/v) surfactant P20] were immobilized on the surface by noncovalent capture to streptavidin. One of the flow cells was left blank in the experiments and served as a control for subtraction. Manual injection was used with 25 nM DNA and a flow rate of 2 μL/min to achieve long contact times with the surface and to control the amount of the DNA bound to the surface. The human G4 DNA folded into a quadruplex in the SPR experiments in the presence of K^+ (BIAcore HBS-EP buffer, filtered and degassed with 0.01 M HEPES at pH 7.4, 0.15 M NaCl, 3 mM EDTA, 0.005% surfactant P20 supplemented with 0.2 M KCl). Folding with respect to time was checked by a series of melting/cooling experiments assessed by both CD and UV methods in solution. All procedures for binding studies were automated by using repetitive cycles of sample injection and regeneration as previously described (*16*, *17*).

All ligand samples were dissolved in DMSO (1 mM) and then diluted as a stock solution to 1×10^{-5} M in the HEPES buffer at pH 7.4. Samples of each were prepared in filtered and degassed buffer that contained a final concentration of 1% DMSO. Different concentrations of the samples were prepared by serial dilution from the stock solutions to keep the DMSO concentration in all samples and the running buffer the same. The same running buffer was used for regeneration of the surface. Samples were injected at a flow rate of 20 μL/min by using the KINJECT command for steady-state experiments. Double-referencing subtractions were used for data analysis. The first reference subtraction eliminates the bulk refractive index change of the injection noise, whereas the second subtraction of a blank buffer injection eliminates any systematic changes that are characteristic of a particular cell (*18*). The results were converted to equilibrium binding constants by using previously described methods (*16*−*19*).

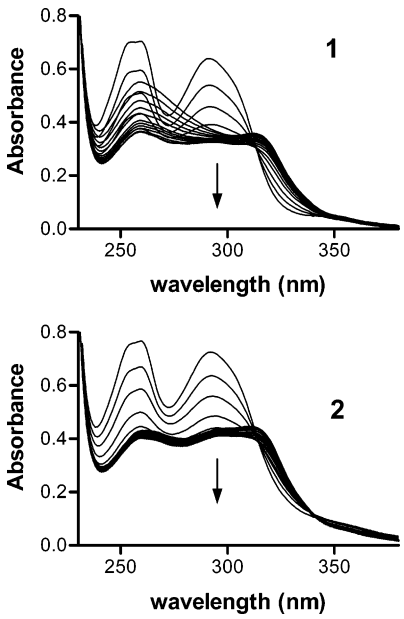

FIGURE 2: DNA titration of **1** and **2**. To 1 mL of drug solution at 20 μM were added aliquots of a concentrated calf thymus DNA solution. The phosphate−DNA/drug ratio increased from 0 to 20 (top to bottom curves, at 260 nm). Measurements were performed in BPE buffer at pH 7.1 (6 mM Na_2HPO_4, 2 mM NaH_2PO_4, and 1 mM Na_2EDTA). Spectra are referenced against DNA solutions of exactly the same DNA concentration and were adjusted to a common baseline.

Topoisomerase Inhibition. The experimental procedure has been previously detailed (*20*). Supercoiled pKMp27 DNA (0.2 μg) was incubated with 4 units of human topoisomerase I/II (TopoGen Inc.) at 37 °C for 1 h in relaxation buffer (10 mM Tris-HCl at pH 7.9, 100 mM NaCl, 1 mM EDTA, 0.1% BSA, 0.1 mM spermidine, and 5% glycerol) in the presence of varying concentrations of the drug under study. Reactions were terminated by adding SDS to 0.25% and proteinase K to 250 μg/mL. DNA samples were then added to the electrophoresis dye mixture (5 μL) and electrophoresed in a 1% agarose gel at room temperature for 2 h at 120 V. Gels were stained with ethidium bromide (1 μg/mL), washed, and photographed under UV light.

RESULTS

Interaction with DNA: Spectral Changes on Complex Formation. (a) UV−*Visible Absorption Spectral Changes and the DNA Melting Temperature Study*. DNA induces significant shifts in the UV−vis spectra of the carbazoles **1**

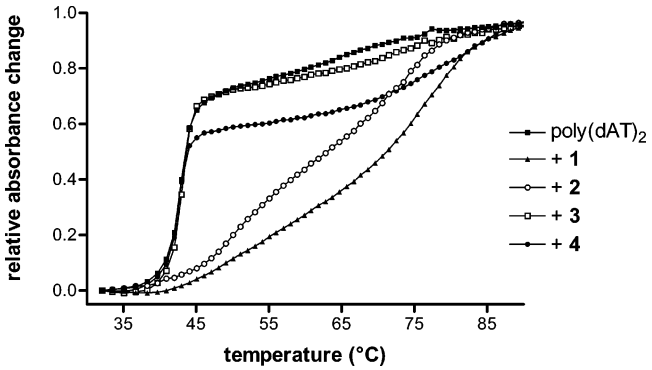

FIGURE 3: Melting temperature variation ΔT_m ($T_m^{\text{drug−DNA complex}} - T_m^{\text{DNA alone}}$, in °C) of poly(dAT)$_2$ after incubation with the diphenylcarbazoles. The T_m measurements were performed at a constant drug/DNA−phosphate ratio of 10 (2 μM drug and 20 μM DNA−nucleotide). T_m measurements were performed in BPE buffer at pH 7.1 (6 mM Na_2HPO_4, 2 mM NaH_2PO_4, and 1 mM EDTA), in 1 cm quartz cuvettes at 260 nm with a heating rate of 1 °C/min. The T_m values were obtained from first-derivative plots.

and **2** (Figure 2). These experiments were performed in BPE buffer, and similar spectral changes were observed when using the cacodylate buffer (as used for the CD and ELD measurements). Addition of calf thymus DNA to both compounds results in a significant decrease in the extinction coefficient at the peak wavelength centered at 260 and 293 nm, and the later peak is shifted to a longer wavelength. In the 260 nm band, the two compounds behave differently. With **2**, the absorbance at 260 nm decreases and then stabilizes at a constant level, whereas with **1**, the decrease is followed by a marked increase as the DNA concentration is increased. There was practically no shift with **3** and only a modest hypochromic shift with **4** (spectra not shown), much weaker than that observed with **1** and **2**. The low capacity of the OH compounds **3** and **4** to interact with DNA was also noticed from the melting temperature (T_m) experiments, where it is obvious that these two uncharged molecules do not augment the T_m of calf thymus DNA, in marked contrast to the cationic derivatives **1** and **2** (Figure 3). These two compounds with two or three dimethylaminoethyl side chains strongly stabilize DNA against heat denaturation. The T_m of the alternating polynucleotide poly(dAT)$_2$ increases from 42 °C to more than 70 °C in the presence of **1** or **2**, at a drug/DNA−nucleotide ratio of 0.1. In fact, the melting curves with both **1** and **2** are biphasic with transition points at 50.3° and 75.4° for **1** and 48° and 71.5° for **2**, as determined from the first derivative plots of the melting curves. There is no doubt that these two compounds bind strongly to DNA, in sharp contrast to the hydroxylated derivatives. Unsurprisingly, the replacement of the terminal OH groups of **4** with dimethylamino groups strongly promotes binding to DNA, and the incorporation of a third dimethylaminoethyl side chain on the carbazole nitrogen further reinforces the capacity of the molecule to interact with its DNA target. The hypochromic and bathochromic shifts observed with **1** and **2** reflect the strong interaction of the diphenylcarbazole aromatic system with DNA base pairs, and the addition of a supplementary side chain directly on the central pyrrole ring must induce a different interaction, which perturbs the orientation of the carbazole system with respect to the DNA base pairs.

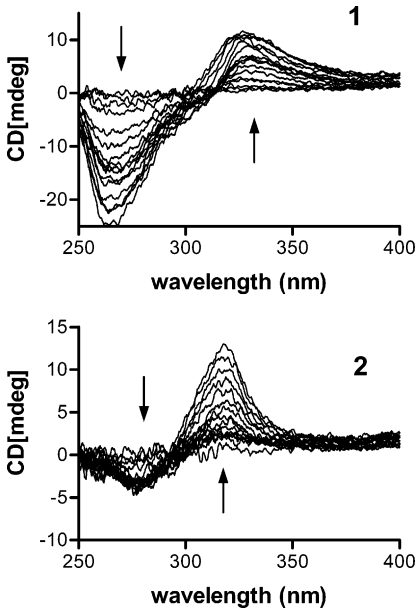

FIGURE 4: CD spectra of **1** and **2** in the presence of graded amounts of calf thymus DNA. DNA titrations of the drugs were performed in 1 mM sodium cacodylate buffer at pH 7.0. To 3 mL of drug solution at 50 μM were added aliquots of a concentrated calf thymus DNA solution. The spectrum of the final complex corresponded to a phosphate−DNA/drug ratio of 20. Arrows point to the spectral changes induced by adding DNA.

(b) CD. CD spectra were recorded at a fixed drug concentration in the presence of increasing amounts of DNA, in both the 250−300 nm region where DNA absorbs and the 300−400 nm region where only the drugs absorb (Figure 4). The positive-induced CD detected with **1** and **2** around 320−330 nm is due to induced CD in the bound carbazole molecules. As with the absorption spectra results, the CD titrations are quite different for **1** and **2**, indicating a distinct orientation of the bound molecules with respect to the DNA-binding pockets. With **3**, there was no induced CD, and the positive CD band at 320 nm was weak with **4** (spectra not shown).

(c) ELD. To evaluate the binding mode, the drug−DNA complexes were oriented in an electric field and the position of the DNA-bound molecules was probed by a linearly polarized light. The ELD spectra of **1** bound to calf thymus DNA, poly(dAT)$_2$, and poly(dGC)$_2$ are very similar and gave negative-reduced dichroism ($\Delta A/A$) signals in the drug absorption band around 320 nm (Figure 5). Negative $\Delta A/A$ signals were obtained with all four compounds, but the magnitude of the ELD values vary significantly from one compound to another. Figure 6 shows the dependence of $\Delta A/A$ on the electric field strength for the four drug−DNA complexes. The values are very weak with **4**, most likely because of the poor affinity of this compound for DNA. Compound **3** bound to DNA gave ELD identical to those recorded with DNA alone, whereas **1** and **2** gave more negative values. The negative ELD signals of intensity equal or superior to those of DNA indicate that the drug molecules are oriented more or less parallel to the plane of the DNA base pair (i.e., perpendicular to the DNA axis or the electric field direction). It is quite frequent that intercalating agents give $\Delta A/A$ values superior to those of DNA, and this is generally attributed to drug-induced structural perturbation of the DNA double helix (*13*). The unwinding of the helix

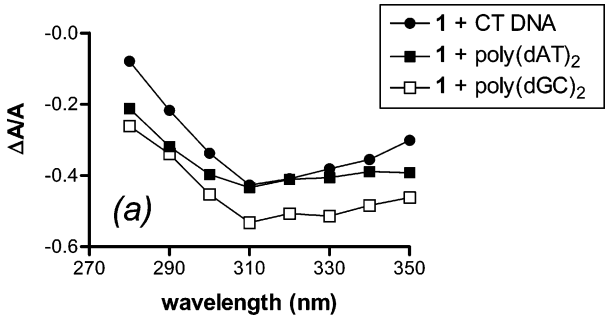

FIGURE 5: ELD spectra of **1** bound to calf thymus DNA or the alternating polymers poly(dAT)$_2$ and poly(dGC)$_2$. ELD spectra were recorded at a 13.5 kV/cm and at a P/D ratio of 25 (250 μM DNA and 10 μM drug), at room temperature (20 °C) in 1 mM sodium cacodylate buffer at pH 7.0.

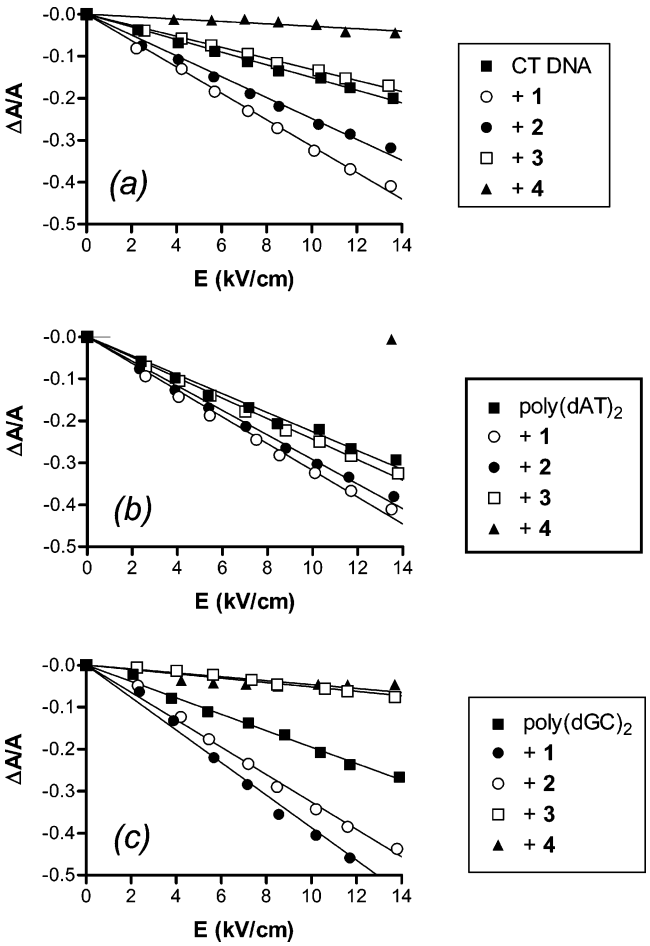

FIGURE 6: Dependence of the reduced dichroism $\Delta A/A$ on the electric field strength for the diphenylcarbazoles bound to (a) calf thymus DNA, (b) poly(dAT)$_2$, or (c) poly(dGC)$_2$. Conditions, P/D = 20 (200 μM DNA and 10 μM drug); 320 nm for the different drug−DNA complexes and 260 nm for the DNA alone. All measurements were performed at room temperature (20 °C) in 1 mM sodium cacodylate buffer at pH 7.0.

induced by the sliding of the drug chromophore between two consecutive base pairs facilitates its orientation in the electric field, and in addition, the drug may also rigidify the macromolecule receptor so as to favor its capacity to orient parallel to the electric field. The results obtained here with the diphenylcarbazole compounds are directly reminiscent to those previously obtained with other series of intercalating agents, in the diphenylfuran series (*21*) and in the carbazole diamidine series for drugs interacting with GC sites (*9*).

Similar ELD experiments were carried out with the alternating polymers poly(dAT)$_2$ and poly(dGC)$_2$ (Figure 6). With the AT polymer, the results are relatively similar to those obtained with calf thymus DNA: a very low level of binding for **4**; **3** behaves like the unbound polymer; and the two other compounds **1** and **2** both give slightly more negative $\Delta A/A$ values. The situation is different with the GC polymer because, in this case, the binding of the two dimethylaminoethyl compounds remains strong, whereas the hydroxyethyl compound **3** now binds weakly to give $\Delta A/A$ values as low as those obtained with **4**. However, in all cases, the $\Delta A/A$ values are negative, suggesting that the compounds can intercalate into both AT and GC sequences, at least under the experimental conditions of the ELD experiments (low ionic strength). From this set of data, binding of the drugs to the minor groove of DNA is totally excluded. Minor-groove binders always give positive $\Delta A/A$ values, as previously reported with diamidine compounds in the carbazole and diphenylfuran series (*9*, *21*).

Sequence Selectivity. The selective recognition of DNA sequences was studied by DNase I footprinting using a 265-bp restriction fragment derived from plasmid pBS. This DNA substrate has been commonly used in footprinting experiments with a great variety of small molecules, both intercalators and groove binders. The electrophoresis gel shown in Figure 7 indicates that only **1** and **2** affect the cleavage of DNA at certain sites by the endonuclease. The uncharged compounds **3** and **4** have no effects on DNase I cleavage, whatever the drug concentration tested, most likely because their affinity for DNA is too low or because the kinetics of binding is too fast to interfere with the access of the enzyme to the DNA. Preferential binding of the two dimethylaminoethyl compounds to different sites along the DNA sequence is clearly revealed by the footprints where the extent of cleavage by the nuclease is reduced. Five drug binding sites were identified with both **1** and **2**, essentially at sequences containing consecutive A−T base pairs but not exclusively. The two molecules recognize the same sequences, but the extent of footprint is slightly higher with **1** compared to **2**. This is more clearly evident from the differential cleavage plots presented in Figure 8. In this type of graph, the negative values refer to sites protected from DNase I cleavage by the test compound, whereas the positive values refer to sites where the cutting of DNA by the nuclease has been promoted by the drug, most likely as a result of drug-induced perturbation of the DNA helix structure, thereby facilitating the access of the enzyme to its cleavage sites. The stimulation of enzymatic cleavage at or adjacent to the ligand-binding site may be indicative of preferred ternary complex (drug−DNA−DNase I) formation. Three of the binding sites coincide with AT stretches (5′-ATTA, 5′-TAAA, and 5′-AAAA). The two other sites, 5′-GCATG and 5′-CTAGA, have no special AT character, and they also correspond to high-affinity receptors for both compounds. It seems that the carbazole molecules can accommodate different sequences. At present, no precise molecular rule can be determined to rationalize these footprinting information. Experiments with a wide range of sequences would be needed to better comprehend the rules that dictate drug binding to DNA.

Biosensor SPR Analysis of DNA Interactions. To quantify the interaction, the binding of the carbazole compounds **1**

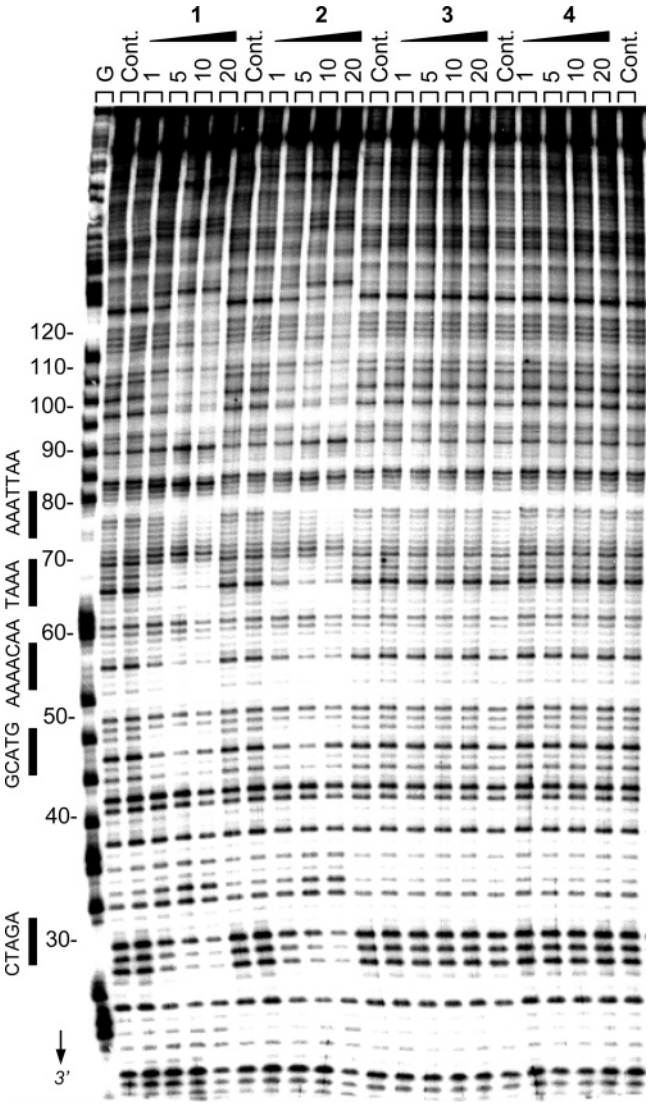

FIGURE 7: DNase I footprinting of **1**−**4** on the 265-bp *Eco*RI−*Pvu*II DNA fragment from pBS. The DNA was 3′-end-labeled with [α-^{32}P]dATP in the presence of AMV reverse transcriptase. The products of nuclease digestion were resolved on an 8% polyacrylamide gel containing 8 M urea. The concentration (micromolar) of the drug is shown at the top of the appropriate gel lanes. Control tracks (Cont.) contained no drug. The track labeled "G" represents dimethylsulfate piperidine markers specific for guanines.

and **2** to DNA was examined by SPR techniques with immobilized oligonucleotides. Parallel experiments were performed with the duplex sequence d(CGAATTCG)$_2$ (in the form of a hairpin) and the telomeric quadruplex sequence d[AG$_3$(TTAG$_3$)$_3$]. The choice of this later sequence derives from the recent work of Chang et al. (*22*), showing that a 3,6-vinylcarbazole structurally related to our carbazoles binds selectively to quadruplex DNA. It was therefore appropriate to evaluate this interaction. Experiments were performed under experimental conditions suitable for G-quadruplex formation. Sensorgrams for the two compounds binding to the human G4 sequence are shown in Figure 9. A relatively large (micromolar) concentration of the compounds was required to yield a significant SPR signal, and saturation of the binding sites was not achieved at the highest concentrations (up to 5 μM) used in the experiments. Similar results were observed for duplex binding. It is clear that these compounds bind significantly more weakly than other compounds, such as a macrocycle (*17*) and ditercalinium (*16*) that we have investigated with these sequences. The increased SPR response with the trication indicates that it binds more strongly than the dication under these conditions, in agreement with the other data. Because of the weak binding, the fitting results have a larger error than with compounds that can approach saturation binding. The best fits were obtained with an equivalent site model with two sites for compound binding to the G4 sequence and 2−3 sites for the duplex (Table 1). The di- and trisubstituted compounds have similar binding constants for the duplex and quadruplex DNAs. As expected, the trisubstituted compound binds more strongly than the disubstituted derivative, but both compounds bind weakly to the duplex and G4 sequences under the high-salt conditions (200 mM K^+) of these experiments.

Effects on Topoisomerases. A conventional DNA relaxation assay was used to investigate the effect of the carbazoles on human DNA topoisomerases. In these experiments, supercoiled DNA was treated with either topoisomerase I or II in the presence of increasing concentrations of the test drug (up to 50 μM) and the DNA relaxation products were then resolved by electrophoresis on agarose gels. Representative gels are shown in Figure 10a (topo I) and Figure 10b (topo II). The drug does not promote DNA cleavage by topoisomerases. No significant increase in the amount of nicked (for topo I) or linear (for topo II) DNA species was observed in the any of the diphenylcarbazoles, in contrast to what is observed with the reference drugs camptothecin and etoposide, which produce a high level of single- or double-strand breaks, respectively. The minor effects observed with **3** and **4** on topoisomerase I and to a lesser extent on topoisomerase II (increase of the nicked DNA band) were not reproducibly observed. These compounds must therefore not be considered as a topoisomerase poisons. However, it is interesting to see once again in these gel experiments that the affinity of the two dimethylamino compounds **1** and **2** is much higher than that of the uncharged analogues **3** and **4**. These two later molecules do not reduce the electrophoretic migration of the supercoiled DNA, in contrast to the analogues with two or three charged branches, which both induce marked gel shifts, and this is also consistent with their efficient intercalative binding to DNA. In fact, when we performed identical gels in the absence of ethidium bromide during electrophoresis (gels stained with ethidium after electrophoresis), we could detect the unwinding of DNA resulting from the intercalation of the drug between base pairs. This is shown in Figure 10c with **2**. The topoisomer population is shifted to the top part of the gel at 5 μM (relaxation) and higher drug concentrations; the DNA becomes positively supercoiled because of intercalation; and then it starts to migrate faster in the gel. Together with the ELD data, this result attests that **2** effectively intercalates into DNA.

DISCUSSION

DNA is a remarkable bioreceptor for a vast number of small molecules (*23*), and it remains a biological target of major interest for the design of anticancer agents (*24*). DNA intercalating agents have been studied for several decades, and a few representatives (anthracyclines, acridines, and anthraquinones) are routinely used in the clinic for the treatment of cancers. DNA minor-groove binders have been

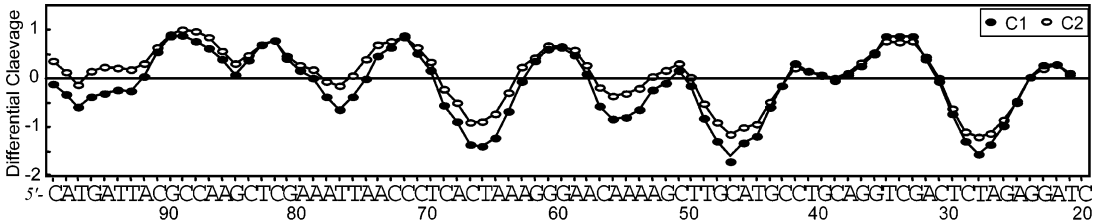

FIGURE 8: Differential cleavage plots comparing the susceptibility of the 265-mer DNA fragment to DNase I cutting in the presence of 20 μM **1** or **2**. Negative values correspond to a ligand-protected site, and positive values represent enhanced cleavage. Vertical scales are in units of ln(fa) − ln(fc), where fa is the fractional cleavage at any bond in the presence of the drug and fc is the fractional cleavage of the same bond in the control, given closely similar extents of overall digestion. Each line drawn represents a three-bond running average of individual data points, calculated by averaging the value of ln(fa) − ln(fc) at any bond with those of its two nearest neighbors. Only the region of the restriction fragment analyzed by densitometry is shown.

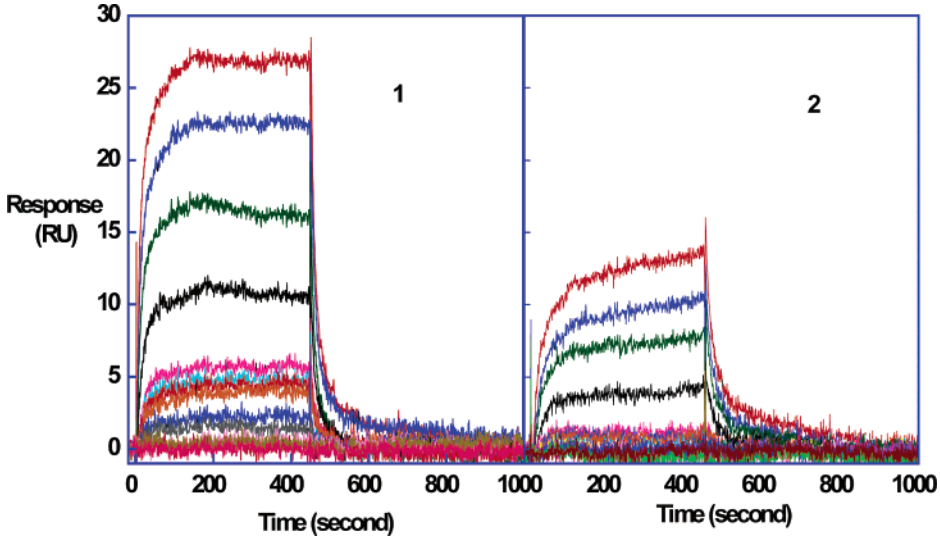

FIGURE 9: Set of SPR sensorgrams for binding of the carbazole compounds **1** and **2** to the human G quadruplex at 25 °C in HEPES buffer. The unbound compound concentrations in the flow solution were 0−5 μM from the lowest curve to the top curve. The lines are linear best fits to the steady-state RU (response unit) values, which are directly proportional to the amount of bound compound, and were used to determine the RU for each free ligand concentration. The RU values from the steady-state region were used to determine binding constants in Table 1.

Table 1: Carbazole Binding Constants to Duplex and Quadruplex DNA[a]

	CGAATTCG	human G4
compound	K	K
1	2.1×10^5	2.3×10^5
2	7.1×10^4	6.0×10^4

[a] Binding results were analyzed with a 2 equiv site model as previously described for G4 interactions (*16*, *17*).

also studied for a long time, but their development as therapeutic agents have met limited success. However, significant progresses have been made recently with the design of diphenylfuran derivatives, which represent promising antiparasitic agents (*25*), and bis/terbenzimidazoles endowed with potent cytotoxic activities (*4*, *26*−*28*). The promising antitumor activity recently reported with a series of head−head bisphenylbenzimidazoles (*1*), coupled with their interesting DNA-binding properties (*2*), prompted us to design a novel series of structurally related DNA-binding agents incorporating a central carbazole unit. The carbazole tricycle has been used to construct DNA minor-groove binders active against different parasites (*7*−*9*), and it is also frequently encountered in DNA-intercalating agents, including inhibitors of topoisomerase I (e.g., indolocarbazole) (*29*) or topoisomerase II (e.g., pyrrolocarbazoles, pyridocarbazoles, and benzopyrimidocarbazoles) (*5*, *30*, *31*). Therefore, a priori, there are good reasons to believe that the diphenylcarbazole aromatic system can represent a DNA-binding template for construction of new therapeutic candidates. The experiments reported here support this idea.

The four diphenylcarbazole derivatives used in the present study exhibit different levels of DNA binding. The two hydroxy compounds **3** and **4** show little interaction with DNA, in contrast to the two analogues equipped with two or three dimethylamino ethyl side chains, which both bind tightly to DNA. This is not surprising because the protonation of the terminal nitrogen at neutral pH must greatly facilitate the interaction with the anionic DNA polymer. The Y-shape compound **1** with three alkyl chains bind slightly more tightly to DNA than the V-shape analogue **2**, but the difference is not large. From the biological point of view, the presence of two side chains is sufficient to confer solubility and activity (**2** is three times more cytotoxic than **1** on P388 cells) (*11*). Similar compounds substituted with a *N*-dimethylaminoalkyl side chain have been reported in the polyamide series (the microgonotropens designed by Bruice and co-workers), but the gain of DNA affinity generally does not correlate with the biological activity (*32*, *33*).

Initially, our goal was to maintain the AT-preference characteristic of most DNA minor-groove binders, in particular, the aforementioned diamidinocarbazoles and bisbenz-

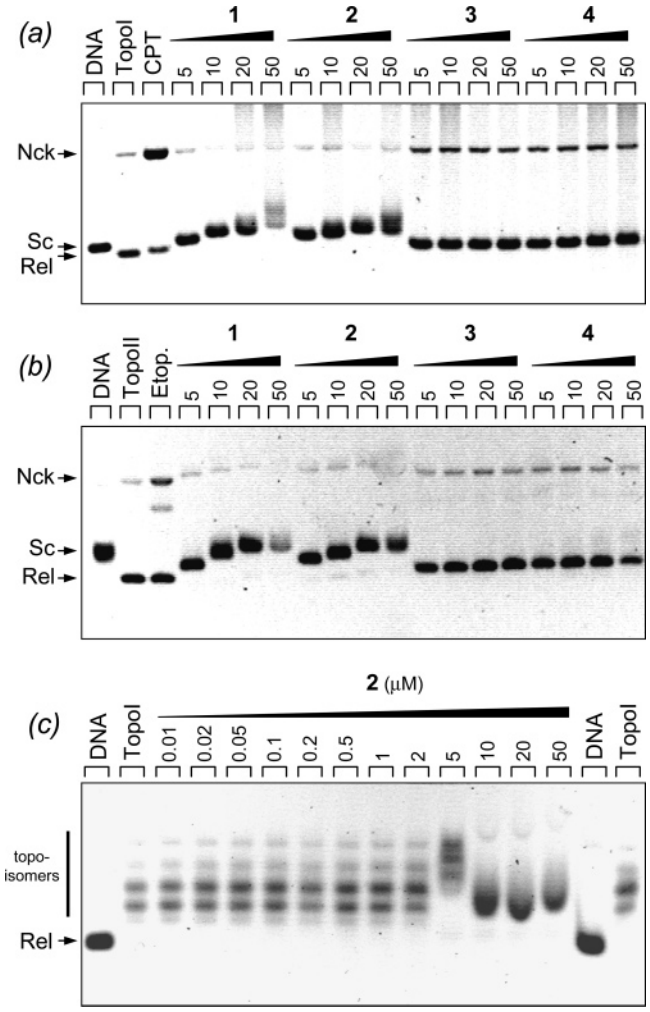

FIGURE 10: Effect of increasing concentrations of the test compounds on the relaxation of plasmid DNA by human topoisomerases I (a) and II (b). Native supercoiled pKMp27 DNA (0.15 μg) (lane DNA) was incubated with 4 units of topoisomerase in the absence (lane Topo) or presence of a given drug at the indicated concentration (micromolar). The camptothecin (lane CPT) and etoposide (lane Etop.) were used at 50 μM. Reactions were stopped with SDS and treatment with proteinase K. DNA samples were separated by electrophoresis on agarose gels containing ethidium bromide (1 μg/mL). (c) Gel performed with topoisomerase I in the presence of increasing concentrations of **2**, and in this case, the DNA samples were run on an agarose gel in the absence of ethidium bromide. This fluorescent dye was added after the electrophoresis by soaking the gel in a solution of ethidium bromide. The gels were photographed under UV light. Nck, nicked; Lin, linear; Rel, relaxed; and Sc, supercoiled DNA.

imidazoles. Interestingly, our diphenylcarbazole still retains a pronounced sequence selectivity, but the sequences preferentially recognized are not exclusively AT-rich. An unusual duality of sites has been identified by DNase I footprinting. Carbazoles **1** and **2** protect DNA from cutting by the enzyme at two types of sequences: AT stretches composed of 4 consecutive A·T base pairs and mixed sequences encompassing two A·T pairs flanked by G·C base pairs (5′-CATG and 5′-CTAG). At present, we have not been able to provide a rational basis for this dual binding preference. The possibility that the carbazoles exhibit two distinct binding modes, minor-groove binding at AT sites and intercalation at (G/C)(AT/TA)(G/C) sites, has been considered, but the ELD measurements do not support this hypothesis. The biphasic curves

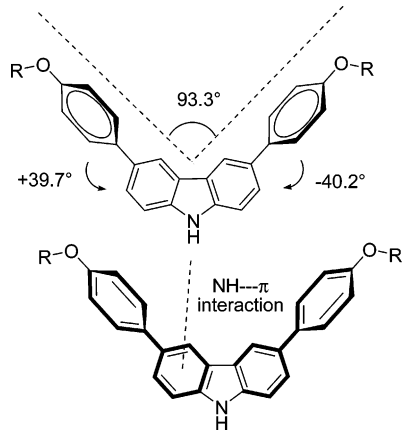

FIGURE 11: Schematic representation of the three-dimensional conformation of the diphenylcarbazole system (adapted from the crystal structure of the methoxy derivative of **3**, as reported in ref *37*).

resulting from the T_m measurements indeed suggest the occurrence of two distinct binding modes to the poly(dAT)$_2$ polymer. At first sight, a groove-binding process could be proposed from the CD measurements because of the positive-induced CD signals measured in the drug absorption band in the presence of DNA. Positive-induced CD is usually a signature of minor-groove binders, but CD data should be interpreted with caution because a slight movement of a chromophore intercalated between base pairs suffices to significantly change the intensity and sign of the induced CD signals (*34*, *35*). The ELD data strongly argue against the implication of a minor-groove-binding process for the diphenylcarbazoles. We always measured negative-reduced dichroism signals with the drug bound to poly(dAT)$_2$ or poly(dGC)$_2$, whereas classical minor-groove binders always give opposite, positive $\Delta A/A$ values under identical experimental conditions (*9*, *21*, *36*). The unwinding of supercoiled DNA induced by compound **2** observed in the experiments with topoisomerase I is also consistent with an intercalative binding mode for this molecule. In fact, the substitution of the central carbazole ring at positions 3 and 6 with the phenyl group confers an important curvature to the compound. which is not well-adapted for an insertion into the narrow minor groove of AT tracts. A crystal structure has been published (*37*) for a diphenylcarbazole structurally equivalent to compound **3** (OH replaced with OCH_3). This methoxy compound, designed as a component for liquid crystals, projects the two phenyl ring at a right angle (93.3° with pseudo $C2v$ symmetry, as depicted in Figure 11), and the two phenyl rings are twisted out of the plane of the central carbazole moiety by +39.7° and −40.2° (Figure 11). These molecules have strong stacking properties that facilitate crystal packing with the formation of key NH$\cdots\pi$ interactions, which stabilize the architecture of the crystal (*37*). The same properties can be invoked to explain the facile intercalation of our diphenylcarbazole between DNA base pairs. The absence of a fully planar aromatic system is not an obstacle for intercalation. There are examples in the literature of nonplanar molecules that adapt their conformation to a pseudoplanar configuration upon binding to DNA (*38*).

The V-shaped diphenylcarbazole system can be viewed as two mesogenic alkoxybiphenyl moieties maintained in a

fixed orientation by a pyrrole (Figure 11). This novel generic structure can be exploited for the recognition of duplex DNA sequences and possibly other DNA structures. Recently, a related 3,6-vinylcarbazole has been characterized as a highly selective ligand for quadruplex DNA (*22*). This observation prompted us to investigate the interaction of **1** and **2** with telomeric quadruplex DNA. We used SPR to evaluate and quantify this interaction, under experimental conditions previously validated with other small molecules interacting with quadruplex DNA (*16*, *17*). In both cases, an interaction was detected but it is weak. For example, the affinity constant for compound **1** interacting with the G4 sequence is 100 times lower than K measured with ditercalinium under strictly identical conditions. Compounds **1** and **2** bind with the same affinity to the human telomeric DNA sequence $d[AG_3(TTAG_3)_3]$ and the $d(CGAATTCG)_2$ duplex. Altogether, the results indicate that the V-shaped diphenylcarbazole system represents a novel pharmacophore for DNA recognition.

REFERENCES

1. Mann, J., Baron, A., Opoku-Boahen, Y., Johansson, E., Parkinson, G., Kelland, L. R., and Neidle, S. (2001) A new class of symmetric bisbenzimidazole-based DNA minor groove-binding agents showing antitumor activity, *J. Med. Chem. 44*, 138−144.
2. Bailly, C., Chessari, G., Carrasco, C., Joubert, A., Mann, J., Wilson, W. D., and Neidle, S. (2003) Sequence-specific minor groove binding by *bis*-benzimidazoles: Water molecules in ligand recognition, *Nucleic Acids Res. 31*, 1514−1524.
3. Joubert, A., Sun, X.-W., Johansson, E., Bailly, C., Mann, J., and Neidle, S. (2002) Sequence selective targeting of long stretches of the DNA minor groove by a novel dimeric bis-benzimidazole, *Biochemistry 42*, 5984−5992.
4. Seaton, A., Higgins, C., Mann, J., Baron, A., Bailly, C., Neidle, S., and van den Berg, H. (2003) Mechanistic and anti-proliferative studies of two novel biologically active bis-benzimidazoles, *Eur. J. Cancer 39*, 2548−2555.
5. Joseph, B., Facompre, M., Da Costa, H., Routier, S., Merour, J. Y., Colson, P., Houssier, C., and Bailly, C. (2001) Synthesis, cytotoxicity, DNA interaction, and topoisomerase II inhibition properties of tetrahydropyrrolo[3,4-*a*]carbazole-1,3-dione and tetrahydropyrido-[3,2-*b*]pyrrolo[3,4-*g*]indole-1,3-dione derivatives, *Bioorg. Med. Chem. 9*, 1533−1541.
6. Mérour, J.-Y., and Joseph, B. (2001) Synthesis and reactivity of 7-azaindole (1*H*-pyrrolo[2,3-*b*]pyridine, *Curr. Org. Chem. 5*, 471−506.
7. Tanious, F. A., Ding, D., Patrick, D. A., Tidwell, R. R., and Wilson, W. D. (1997) A new type of DNA minor groove complex: Carbazole dication−DNA interactions, *Biochemistry 36*, 15315−15325.
8. Tanious, F., Ding, D., Patrick, D. A., Bailly, C., Tidwell, R. R., and Wilson, W. D. (2000) Effects of compound structure on carbazole dication−DNA complexes: Tests of the minor-groove complex models, *Biochemistry 39*, 12091−12101.
9. Tanious, F. A., Wilson, W. D., Patrick, D. A., Tidwell, R. R., Colson, P., Houssier, C., Tardy, C., and Bailly, C. (2001) Sequence-dependent binding of bis-amidine carbazole dications to DNA, *Eur. J. Biochem. 268*, 3455−3464.
10. Soderlind, K. J., Gorodesky, B., Singh, A. K., Bachur, N. R., Miller, G. G., and Lown, J. W. (1999) Bis-benzimidazole anticancer agents: Targeting human tumour helicases, *Anti-Cancer Drug Des. 14*, 19−36.
11. Jacquemard, U., Routier, S., Tatibouët, A., Kluza, J., Laine, W., Bal, C., and Bailly, C. (2004) Synthesis of diphenyl-carbazoles as cytotoxic DNA binding agents, *Org. Biomol. Chem. 2*, 1476−1483.
12. Houssier, C., and O'Konski, C. T. (1981) Electro-optical instrumentation systems with their data acquisiton and treatment, in *Molecular Electro-optics* (Krause, S., Ed.) pp 309−339, Plenum Publishing Corporation, New York.
13. Colson, P., Bailly, C., and Houssier, C. (1996) Electric linear dichroism as a new tool to study sequence preference in drug binding to DNA, *Biophys. Chem. 58*, 125−140.
14. Bailly, C., Kluza, J., Ellis, T., and Waring, M. J. (2004) DNase I footprinting of small molecule binding sites on DNA, *Methods Mol. Biol. 288*, 319−342.
15. Bailly, C., and Waring, M. J. (1995) Comparison of different footprinting methodologies for detecting binding sites for a small ligand on DNA, *J. Biomol. Struct. Dyn. 12*, 869−898.
16. Carrasco, C., Rosu, F., Gabelica, V., Houssier, C., De Pauw, E., Garbay-Gaureguiberry, C., Roques, B., Wilson, W. D., Chaires, J. B., Waring, M. J., and Bailly, C. (2002) Tight binding of the antitumor drug ditercalinium to quadruplex DNA, *ChemBioChem 3*, 1235−1241.
17. Teulade-Fichou, M. P., Carrasco, C., Guittat, L., Bailly, C., Alberti, P., Mergny, J. L., David, A., Vigneron, J. P., Lehn, J. M., and Wilson, W. D. (2003) Selective recognition of G-quadruplex telomeric DNA by a bis-quinacridine macrocycle, *J. Am. Chem. Soc. 125*, 4732−4740.
18. Myszka, D. G. (1999) Improving biosensor analysis, *J. Mol. Recognit. 12*, 279−284.
19. Davis, T. M., and Wilson, W. D. (2000) Determination of the refractive index increments of small molecules for correction of surface plasmon resonance data, *Anal. Biochem. 284*, 348−353.
20. Bailly, C. (2001) DNA relaxation and cleavage assays to study topoisomerase I inhibitors, *Methods Enzymol. 340*, 610−623.
21. Wilson, W. D., Tanious, F. A., Ding, D., Kumar, A., Boykin, D. W., Colson, P., Houssier, C., and Bailly, C. (1998) Nucleic acid interactions of unfused aromatic cations: Evaluation of proposed minor-groove, major-groove, and intercalation binding modes, *J. Am. Chem. Soc. 120*, 10310−10321.
22. Chang, C.-C., Wu, J.-Y., Chien, C.-W., Wu, W.-S., Liu, H., Kang, C.-C., Yu, L.-J., and Chang, T.-C. (2003) A fluorescent carbazole derivative: High sensitivity for quadruplex DNA, *Anal. Chem. 75*, 6177−6183.
23. Demeunynck, M., Bailly, C., and Wilson, W. D. (2003) *DNA and RNA Binders*, Wiley−VCH, New York.
24. Hurley, L. H. (2002) DNA and its associated processes as targets for cancer therapy, *Nat. Rev. Cancer 2*, 188−200.
25. Tidwell, R. R., and Boykin, D. W. (2003) Dicationic DNA minor groove binders as antimicrobial agents, in *DNA and RNA Binders* (Demeunynck, M., Bailly, C., and Wilson, W. D., Eds.) pp 414−460, Wiley−VCH, New York.
26. Kim, J. S., Sun, Q., Yu, C., Liu, A., Liu, L. F., and LaVoie, E. (1998) Quantitative structure−activity relationships on 5-substituted terbenzimidazoles as topoisomerase I poisons and antitumor agents, *Bioorg. Med. Chem. 6*, 163−172.
27. Xu, Z., Li, T.-K., Kim, J. S., LaVoie, E., Breslauer, K. J., Liu, L. F., and Pilch, D. S. (1998) DNA minor groove binding-directed poisoning of human DNA topoisomerase I by terbenzimidazoles, *Biochemistry 37*, 3558−3566.
28. Jin, S., Kim, J. S., Sim, S.-P., Liu, A., Pilch, D. S., Liu, L. F., and LaVoie, E. J. (2000) Heterocyclic bibenzimidazole derivatives as topoisomerase I inhibitors, *Bioorg. Med. Chem. Lett. 10*, 719−723.
29. Bailly, C., Chessari, G., Carrasco, C., Joubert, A., Mann, J., Wilson, W. D., and Neidle, S. (2003) Sequence-specific minor groove binding by *bis*-benzimidazoles: Water molecules in ligand recognition, *Nucleic Acids Res. 31*, 1514−1524.
30. Bailly, C. (2003) Targeting DNA and topoisomerase I with indolocarbazole antitumor agents, in *Small Molecule DNA and RNA Binders* (Demeunynck, M., Bailly, C., and Wilson, W. D., Eds.) Vol. 2, pp 538−575, Wiley−VCH, New York.
31. Nakamura, K., Sugumi, H., Yamaguchi, A., Uenaka, T., Kotake, Y., Okada, T., Kamata, J., Niijima, J., Nagasu, T., Koyanagi, N., Yoshino, H., Kitoh, K., and Yoshimatsu, K. (2002) Antitumor activity of ER-37328, a novel carbazole topoisomerase II inhibitor, *Mol. Cancer Ther. 1*, 169−175.
32. Nakamura, K., Taniguchi, T., Funahashi, Y., and Yoshimatsu, K. (2003) Effects of ER-37328 on primary tumor, liver metastasis, and life span in a murine colon 38 orthotopic transplantation model, *Mol. Cancer Ther. 2*, 59−64.
33. He, G.-X., Browne, K. A., Blaskò, A., and Bruice, T. C. (1994) Microgonotropens and their interactions with DNA. 4. Synthesis of the tripyrrole peptides tren-microgonotropen-a, -b, and -c and characterization of their interactions with dsDNA, *J. Am. Chem. Soc. 116*, 3716−3725.

34. He, G.-X., Browne, K. A., Groppe, J. C., Blaskò, A., Mei, H.-Y., and Bruice, T. C. (1993) Microgonotropens and their interactions with DNA. 1. Synthesis of the tripyrrole peptides dien-microgonotropen-a, -b, and -c and characterization of their interactions with dsDNA, *J. Am. Chem. Soc. 115*, 7061−7071.
35. Lyng, R., Rodger, A., and Nordén, B. (1991) The CD of ligand−DNA systems. I. poly(dG-dC) B-DNA, *Biopolymers 31*, 1709−1720.
36. Lyng, R., Rodger, A., and Nordén, B. (1992) The CD of ligand−DNA systems. II. poly(dA-dT) B-DNA, *Biopolymers 31*, 1201−1215.
37. Ji, Y. H., Bur, D., Hasler, W., Bailly, C., Waring, M. J., Hochstrasser, R., and Leupin, W. (2001) Tris-benzimidazole derivatives: Design, synthesis, and DNA sequence recognition, *Bioorg. Med. Chem. 9*, 2905−2919.
38. Belloni, M., Manickam, M., Ashton, P. R., Kariuki, B. M., Preece, J. A., Spencer, N., and Wilkie, J. (2001) The X-ray crystal structures and computational analysis of NH···π hydrogen bonded banana-shaped carbazole derivatives and thermal analysis of higher mesogenic homologues, *Mol. Cryst. Liq. Cryst. 369*, 17−35.
39. Woo, S. H., Sun, N. J., Cassady, J. M., and Snapka, R. M. (1999) Topoisomerase II inhibition by aporphine alkaloids, *Biochem. Pharmacol. 57*, 1141−1145.

BI048474O